

# Interharmonics injected into power system by a squirrel-cage induction machine in normal and faulty operating conditions

Jan Rusek

Chair of Electrical Machines

AGH University of Science and Technology

Al. Mickiewicza 30, 30-059 Krakow (Poland)

phone: +48 126172897, fax: +48 126341096, e-mail: [gerusek@cyf-kr.edu.pl](mailto:gerusek@cyf-kr.edu.pl)

**Abstract.** The paper aims at examining interharmonics injected into the power supply system by a healthy and faulty squirrel cage induction machine operated at steady state. The faulty operation discussed encompasses breaks in squirrel cage bars, breaks in squirrel cage end ring segments, combined static and dynamic eccentricity, clutch wobbling and vibration of bearings. The effect of these ailments is first investigated through simulations accomplished with a specially developed and implemented squirrel cage induction machine polyharmonic model, as the fundamental harmonic models are not capable of simultaneous accounting for eccentricities, slotting and actual winding configuration. Two case studies, based on preregistered currents of big industrial machines, confirm the frequencies of interharmonics predicted by theory and simulations. The case studies refer to broken bars and clutch wobbling. The case study analyses were accomplished with the system *Sp4* developed for offline diagnoses of induction machines.

## Key words

Polyharmonic model, spectral composition of currents, interharmonics.

## 1. Introduction

Interharmonics injected by the load into power supply system are cumbersome to eliminate via filtration [1] as they change their frequency, depending on the load conditions. Among many apparatuses capable of generating interharmonics are squirrel cage induction machines. As these machines are the most widespread driving units in both the heavy and light industry, investigation of interharmonics they can generate in normal and faulty operating conditions is an acute issue [2].

Spectral composition of the currents is obtained through Fourier analysis, whereby nowadays this analysis is accomplished almost exclusively in digital domain. The real currents are registered via specialized computers equipped with analog-to-digital converters. Explanations of the spectra for registered currents would require performing similar spectral analysis for calculated currents, that is the currents resulting from computer simulations. Alas, performing such simulations had to be based on the model of the squirrel cage induction machine accounting for cage asymmetry, static, dynamic or mixed eccentricity, vibrations of bearings, clutch wobbling. Obviously, the model should account for

higher harmonics of self and mutual inductances. Such a refined model is usually referred to as diagnostic model of the induction machine. The calculations based on a classical or fundamental harmonic model would be useless with regard to interharmonics. Hence, development of the specialized model, as well as its computer implementation, capable of accounting for the above listed ailments, was a prerequisite for investigations of interharmonics generated by induction machines.

The aim of the contribution is to present spectral compositions of stator currents received from simulations based on the above mentioned specialized model, whereby the simulations have been done successively for each of the listed ailments. To match the real supply conditions, the supply voltage for simulations was assumed to contain not only the 50 hertz fundamental component of  $1000 V_{\text{rms, phase-to-phase}}$  but also the 3<sup>rd</sup>, 5<sup>th</sup> and 7<sup>th</sup> harmonics. The rated power of the wye configured machine was  $P_N = 132 \text{ kW}$ , the number of pole pairs  $p = 2$ , the speed  $n = 1475 \text{ r.p.m.}$ , the number of slots  $N_S/N_R = 72/56$ , the rotor inertia  $J = 4.52 \text{ kgm}^2$  and the inertia of the load  $J_L = 0.52 \text{ kgm}^2$ . To prevent the torsions depending on the clutch stiffness from influencing the current spectra, the clutch was assumed to be perfectly stiff, except in paragraph 7 referring to clutch wobbling. The loading torque was assumed to depend on the square of the rotor speed and to amount to 841 Nm at synchronous speed. The rated torque is 855 Nm.

The case studies refer to 320 kW and 850/450 kW machines, operated in one of the power plants.

## 2. Healthy machine

Fig. 1 shows the starting current followed by the steady-state current, obtained from simulations for the case of perfectly healthy machine.

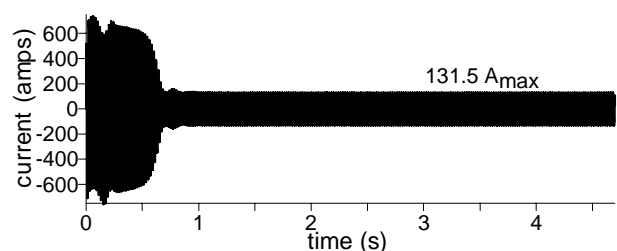


Fig.1. Calculated start up and steady-state current for healthy machine. Sampling period  $T_s = 0.002 \text{ s}$ .

The purposefully prolonged steady-state operation allowed to calculate spectral composition for the steady state segment of the current in Fig. 1. It is presented in Fig. 2.

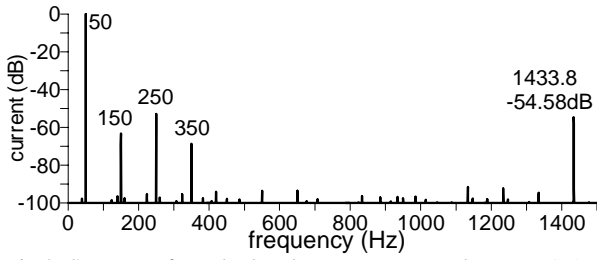


Fig.2. Spectrum for calculated current segment between 1.5 and 4.7 s. Frequency resolution  $\Delta f = 0.3125$  hertz.

The harmonic labeled with 50 is a fundamental harmonic, the steady state amplitude of which is  $131.5 A_{max}$ , as already shown in Fig. 1. The harmonics labeled as 150, 250 and 350 are the 3<sup>rd</sup>, 5<sup>th</sup> and 7<sup>th</sup> harmonics flowing through the machine due to the common supply voltage deformation, accounted for in calculations. The interharmonic labeled as 1433.8 is a main slot harmonic, the frequency of which depends on current rotor speed of the machine. Its magnitude is comparable with that of 5<sup>th</sup> harmonic.

### 3. Broken cage bar

Broken bars result in resistance magnification of the inflicted bar [3]. As bare cage bars are embedded directly in rotor iron, even total fracture of the bar cause resistance magnification by only limited multiplication factor. Its value depend on the shape of the bar cross section. For further calculations the most typical multiplication factor of 20 will be assumed. Fig. 3 presents spectrum of the steady state current segment, similar to that in Fig. 1 but for the rotor with one broken bar, out of 56 total.

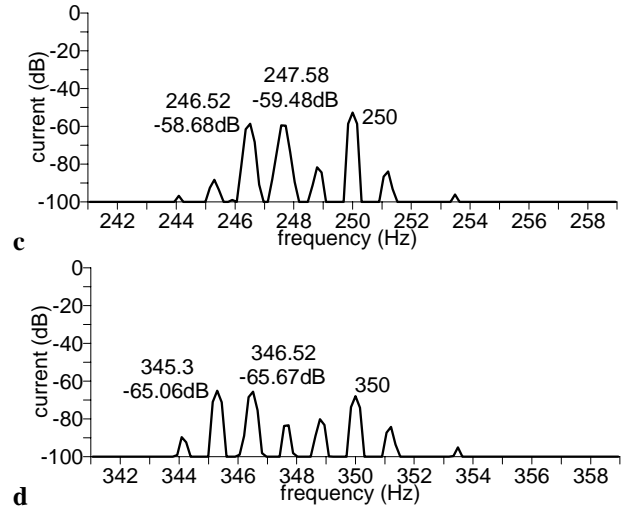
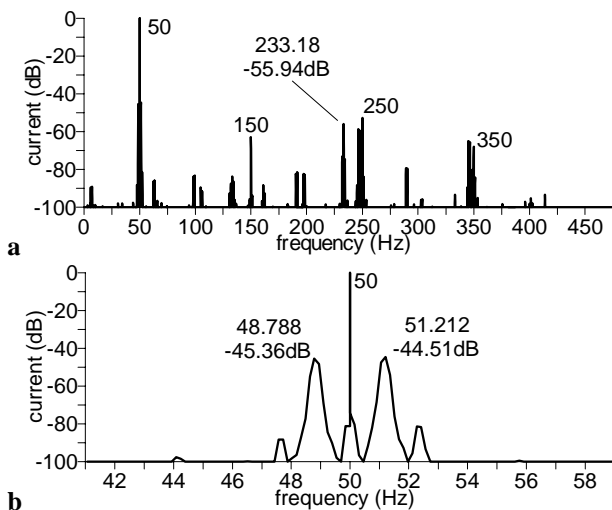


Fig. 3. **a**: Spectrum for calculated current segment between 1.5 and 8.1 s. Resolution  $\Delta f = 0.151515$  Hz. **b**, **c**, **d**: zooms around 50, 250 and 350 Hz. Resistance of one bar multiplied by 20.

The frequency range of the spectrum in Fig. 3 is limited to 450 hertz. The zoom around 50 Hz shows up the pair of new interharmonics injected into power supply system. Their frequencies are 48.788 and 51.212 Hz, for the rotor speed resulting from full load of almost 841 Nm. The frequencies of other interharmonics in Fig. 3a, b, c or d also depend on rotor speed.

### 4. Frequency of diagnostic components

The presence of diagnostic components in Fig. 3b can be justified in the following manner [4]. For the machine operated in steady state the rotor angular speed  $\omega$  can be expressed by

$$\omega = (1-s) \frac{\Omega}{p} = (1-s) \frac{2\pi f_0}{p} \quad (1)$$

where  $s$  - slip,  $\Omega$  - angular frequency of the supply voltages,  $p$  - number of pole pairs,  $f_0$  - supply frequency. The frequency  $f_r$  of the rotor currents is

$$f_r = s f_0 \quad (2)$$

Broken bar results in that its current diminishes. The current attenuation in the inflicted bar can be modeled by superposition of the healthy current with an additional one, so chosen, that its superposition with the former one results in a real current. This artificially injected current will flow through both end rings and one or two adjacent bars to the left and right from the inflicted one. Its frequency is given by (2). This current will produce a number of pulsating components of air gap magnetic flux. The flux component of exactly  $p$  pole pairs will induce electromotive forces in stator windings. The wave of the air gap magnetic flux density of this very component can be expressed qualitatively by

$$B_{Add,R}(y,t) = I_{Add,mx} \cos(s\Omega t) \Lambda \sin(py) \quad (3)$$

or by

$$B_{Add,R}(y,t) = B_{Add,mx}[\sin(py - s\Omega t) + \sin(py + s\Omega t)] \quad (4)$$

where  $A$  is a proportionality coefficient between the current and the magnetic flux density, and  $y$  is a rotor referred circumferential coordinate starting at broken bar. It follows from (4) that the additional flux can be interpreted as a superposition of two flux waves rotating with the rotor referred angular speed of (5) and (6).

$$\omega_{R1} = s \frac{\Omega}{p} \quad (5)$$

$$\omega_{R2} = -s \frac{\Omega}{p}. \quad (6)$$

Considering the angular speed of the rotor itself, the speeds (5) and (6) are equivalent to the stator referred speeds of (7) and (8).

$$\omega_{S1} = \omega + \omega_{R1} = \frac{\Omega}{p} \quad (7)$$

$$\omega_{S2} = \omega + \omega_{R2} = (1-2s) \frac{\Omega}{p}. \quad (8)$$

Wave (7) will induce in the stator winding an additional current of the angular frequency of  $\Omega$ . As this frequency coincides with that of the fundamental current it is useless for diagnostic purposes. To the contrary, the wave of the speed (8) will induce in the stator winding the current the frequency of which differs from that of the fundamental current component. Considering that the stator winding has  $p$  pole pairs, the flux wave of the angular frequency (8) will induce in the stator winding the current component of the frequency (9).

$$f_{S2} = (1-2s) \cdot f_0 \quad (9)$$

However, spectral analyses of the stator currents of the real stationary operated machines reveal that they also contain the harmonic of the angular frequency of (10).

$$f_{S3} = (1+2s) \cdot f_0 \quad (10)$$

The harmonics of the frequencies (9) and (10) will appear below and above the fundamental component, whereby their frequencies will differ from that of the fundamental one by the so called double slip frequency of  $2 \cdot s \cdot f_0$ . The main reason for the current component (10) is speed fluctuation following cage asymmetry. The frequency of the pulsating torque component is just the double slip frequency  $2 \cdot s \cdot f_0$ .

Frequencies (9) and (10) are just the ones seen in Fig. 3b to the left and right of the fundamental or 50 hertz component. Their frequencies are 48.788 and 51.212 hertz.

## 5. Broken segment in one cage end ring

Fractures in rotor cage end rings cause serious asymmetry of current distribution in end ring segments, as the phenomenon of iron shunting does not refer to the

by air surrounded end rings. Hence, the resistance multiplication factor mapping broken end ring segments are much greater than those referring to broken cage bars. In the following the multiplication factor of 200 was assumed. Fig. 4. presents the spectrum for one broken segment in one end ring.

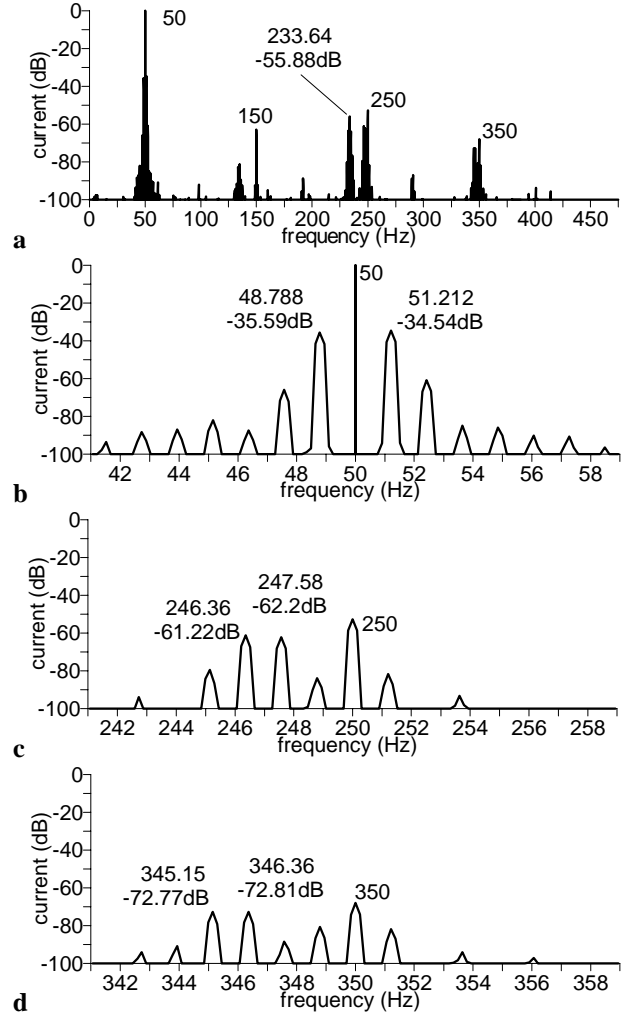


Fig. 4. a: Spectrum for the calculated current segment between 1.5 and 8.1 s. Resolution  $\Delta f = 0.151515$  Hz. b, c, d: zooms around 50, 250 and 350 Hz. Resistance of one segment multiplied by 200.

Spectra in Fig. 3 and 4 are very close to each other. However, in Fig. 4 the interharmonics around 50 Hz are greater those than those in Fig. 3. Contrary to that, in Fig. 4 the interharmonics around 250 and 350 Hz are smaller than those in Fig. 3. Similarly as in Fig. 3, the frequencies of interharmonics produced by the machine and injected into power supply system depend on rotor speed.

## 6. Static plus dynamic eccentricity

One of the common ailments, though not preventing the machine from further prolonged operation, is eccentricity. Dynamic eccentricity consists in that the axis around which the rotor rotates does not coincide with the middle of rotor cross section. Another words, dynamic eccentricity consists in that the axis of rotation is shifted from rotor geometrical center. Static

eccentricity is displacement of the axis of rotation from the geometrical center of stator cross section. By lack of both the static and dynamic eccentricities the axis of rotor rotation coincides with the centers of both the stator and rotor cross sections. The spectrum in Fig. 5 refers to the steady state interval from 1.5 to 4.7 s, by mixed eccentricity of 30 % static plus 30 % dynamic ones.

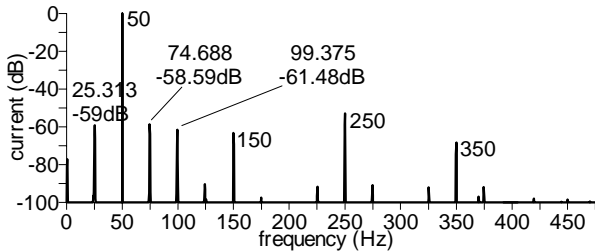


Fig. 5. Spectrum for the calculated current segment between 1.5 and 4.7 s. Resolution  $\Delta f = 0.3125$  Hz. Both static and dynamic eccentricities amount to 30 % of geometrical air gap length.

It follows from Fig. 5 that the mixed eccentricity is accompanied by a pair of interharmonics around the 50 hertz fundamental harmonic. The distance of these harmonics from the fundamental one is the same and amounts to the rotor speed expressed in revolutions per second. The steady state speed varies between 155.262 and 155.267 rad/s. Thus the middle steady state speed is 155.2645 rad/s, what is tantamount to 24.71 rev/s. The predicted frequencies of the above mentioned pair of rotational interharmonics are  $50 - 24.71 = 25.29$  and  $50 + 24.71 = 74.71$  Hz. Considering the frequency resolution of 0.3125 Hz, these frequencies coincide with those of 25.314 and 74.688 Hz seen in Fig. 5.

## 7. Clutch wobbling

Misalignment or skew of the motor and load shafts cause the clutch to produce additional fluctuating torque component acting on both involving shafts. This torque component causes the motor and load rotors to accelerate and decelerate by turns, depending on angular position of the clutch, assumed to be the average of motor and load rotor angular positions. In effect, the rotor speed will fluctuate or wobble. It was assumed that the wobbling torque amounts to 2 % of the clutch nominal torque of 2565 Nm. The latter value amounts to three rated torques of the motor. Here the clutch was assumed to possess the limited stiffness of 90 000 Nm/rad and the nonlinearity factor of 0.9, what causes the clutch characteristic to be parabolic. Fig. 6 shows the spectrum of the steady state current interval of 1.5 to 4.7 s.

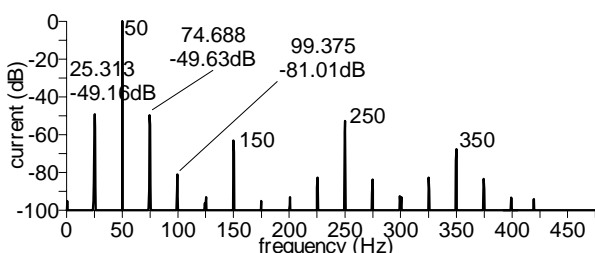


Fig. 6. Spectrum for the calculated current segment between 1.5 and 4.7 s. Resolution  $\Delta f = 0.3125$  Hz. The clutch wobbling amounts to 2 % of the clutch nominal torque of 2565 Nm.

Frequencies of interharmonics in Fig. 6 depend on rotor speed. The spectrum in Fig. 6 is, qualitatively, very close to that in Fig. 5. The most conspicuous quantitative difference between these spectra is the magnitude of the 99.375 Hz interharmonic. In Fig. 5 its magnitude is comparable with that of the 74.688 Hz interharmonic, whereas in Fig. 6 it is much smaller.

## 8. Vibration of bearings

Ailments of bearings may consist in damage of either the rolling element or external or internal bearing race. Either would cause the rotor to vibrate radially in addition to its rotational movement. In calculations it was assumed that these radial vibrations preserve parallelism of stator and rotor axes. Further, it was assumed that each full rotor revolution is accompanied by eight radial vibrations of the amplitude of 40 % of the geometrical air gap. The spectrum of the steady state current is given in Fig. 7.

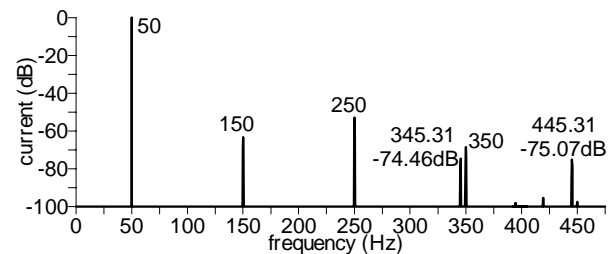


Fig. 7. Spectrum for the calculated current segment between 1.5 and 4.7 s. Resolution  $\Delta f = 0.3125$  Hz. Eight radial swings of the rotor, of the amplitude of 40% of air gap length, per one rotor revolution.

It follows from Fig. 7 that the radial vibrations of the rotor, due to faulty bearings, produce two additional harmonics, the frequencies of which are 345.31 and 445.31 hertz, of comparable amplitude reaching -74.46 and -75.07 dB with respect to 50 hertz fundamental harmonic. However, the frequencies of these harmonics depend on geometrical profile of the bearings, such as diameters of the races and the number of balls or rollers. Likewise, they depend on whether the ball or the race is damaged. For the purpose of this article, the important thing is that the frequencies of these interharmonics depend on rotor speed, what actually makes them nominated to interharmonics.

## 9. Case study - broken bars

Fig. 8. presents a diagnostic report for a 320 kW machine operated in steady state conditions at partial load. The report is produced automatically by a system *Sp4* making use of the pre-registered currents [5]. Actually the current in a secondary side of a current transformer has been registered via current clips. The analog-to-digit converting card onboard of a portable computer performed the registration. The thus registered currents were offline loaded by the *Sp4* diagnostic system. The presence of the additional components around a 50 hertz fundamental component is clearly visible. These harmonics coincide qualitatively with those predicted by calculations and presented in Fig. 3b.

Fig. 8 confirms that broken bars cause that a pair of twin harmonics is injected into power supply system. In the case presented in Fig. 8, the amplitudes of these harmonics amount to 1.5% by 49.16 hertz and 0.85% by 50.72 hertz of the fundamental component, whose amplitude is 36.2 Amx by 49.95 hertz. The slip of

0.778% was established relying on a slot harmonic marked with a square in the vicinity of 900 hertz in plot number two of Fig. 8. The distance of both diagnostic components from the fundamental one is  $2 \cdot s \cdot f_0 = 2 \cdot 0.778 / 100 \cdot 49.95 = 0.777$  hertz. This theoretical distance is confirmed in Fig. 8 with satisfactory accuracy.

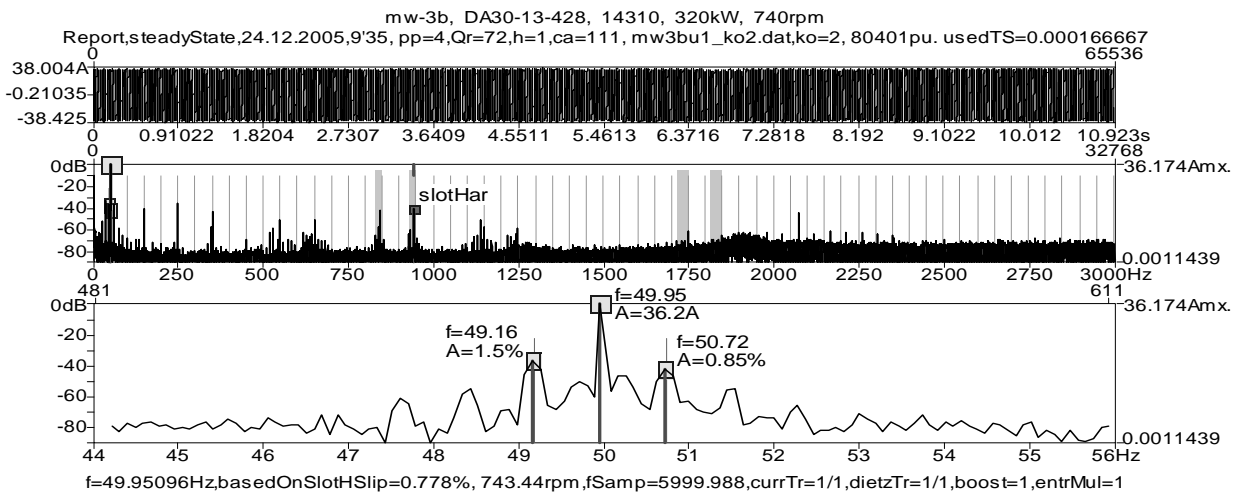


Fig. 8. Diagnostic interharmonics around the 50 hertz fundamental component, due to broken bars in the industrial machine.

## 10. Case study - clutch wobbling

Fig. 9 refers to a double speed machine of 850/450 kW rated power, operated at lower speed that is by 5 pole pairs. It drives a flue gas exhauster in one of the power generating stations. The analysis was done with the *Sp4* diagnostic system for the pre-registered supply current [5]. Irregular load, caused for example by nonalignment of motor and exhauster axes, or by non-uniform

sediments on exhauster's blades, referred to as clutch wobbling, will cause the injection into power supply system a pair of twin rotational harmonics. In the case presented in Fig. 9 their amplitudes are 5.58% by 40 hertz and 5.12% by 59.94 hertz, with respect to the fundamental current component whose amplitude is 53 Amx by 49.97 hertz. Comparing Figures 8 and 9 it can be concluded that clutch wobbling will be accompanied by much higher harmonics injected into power supply system than broken bars.

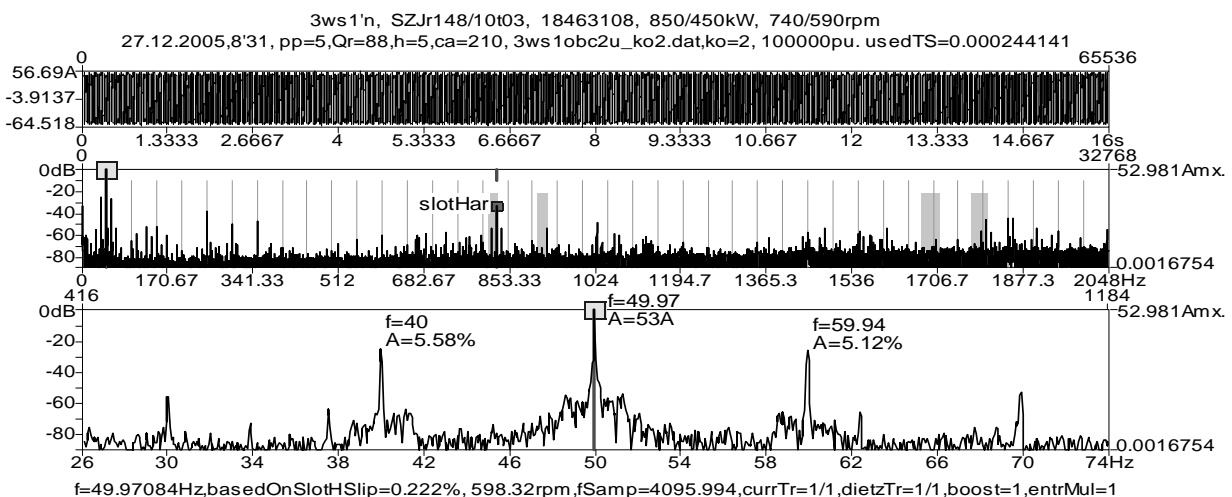


Fig. 9. Rotational interharmonics around the 50 hertz fundamental component, due to clutch wobbling in the industrial machine.

## 11. Conclusions

1. Calculated spectra of the current drawn by a stationary operated squirrel cage induction machine confirm, that this machine, both in healthy and faulty conditions, injects interharmonics into power supply system. In healthy conditions the most important interharmonic is the so called slot harmonic. In faulty conditions

additional interharmonics pop up, especially in lower frequency range. Though in some cases their amplitude may reach -35 dB (e.g. in Fig. 4), usually their amplitude is smaller than -50 dB. However, in the case of bigger machines their amplitudes expressed in amperes can achieve the values being able to deform the substation voltage, resulting in that the polluted voltage would be delivered also to other energy recipients. This, in turn,

cause that the interharmonics injected into the power system by one recipient begin to flow through other recipients supplied by the same substation. Hence, it is not an easy matter to identify which machine is a real source of certain interharmonics, provided several machines operate in parallel while fed from the same substation bus.

2. The developed and implemented "diagnostic model" *As2* proved to be capable to properly simulate various ailments in squirrel cage induction machines. It was indispensable, that it accounts for higher harmonics of both the stator and rotor self and mutual inductances.

3. The developed and implemented diagnostic system *Sp4* proved to be a convenient tool to identify and interpret the spectral composition for in the industry registered currents.

### **Acknowledgement**

This work was supported by AGH University of Science and Technology *Statute Work* number 11.11.120.608.

### **References**

- [1] J. Tlustý, V. Valouch, "Connection of shunt active power filters in multibus industrial power system for harmonic voltage mitigation", in *Proc. ICREPQ'05, Zaragoza* 16-18. 03.2005, pp. 23-24.
- [2] J. Rusek, "Transients in wind-mill driven, two-speed, squirrel-cage induction generator", in *Proc. ICREPQ'05, Zaragoza* 16-18. 03.2005, pp. 19-20.
- [3] W. Rams, J. Rusek, "Practical Diagnosis of Induction Machines Operated in Power Plant Auxiliaries ", in 2005 IEEE St. Petersburg PowerTech Proceedings, St. Petersburg 27-30.06.2005.
- [4] J. Rusek, "Categorization of induction machines in current signature analysis", in *Electrical Engineering* 84 (2002) 265 - 273.
- [5] Database of registered currents, in possession of the Chair of Electrical Machines of the AGH University of Science and Technology, Krakow.